Eur. Phys. J. C (2025) 85:988
https://doi.org/10.1140/epjc/s10052-025-14719-4

THE EUROPEAN PHYSICAL JOURNAL C

Regular Article - Theoretical Physics

Scalar clouds around Melvin–Kerr black holes

Haryanto M. Siahaan[a]

Program Studi Fisika, Universitas Katolik Parahyangan, Jalan Ciumbuleuit 94, Bandung 40141, Indonesia

Received: 12 May 2025 / Accepted: 3 September 2025

Abstract In this paper, we investigate the existence of stationary scalar clouds in the magnetized Kerr black hole background within the framework of Einstein–Maxwell theory. We consider the dynamics of a massive, charged test scalar field governed by the Klein–Gordon equation. Under the assumption of a weak magnetic field, we demonstrate that the Klein–Gordon equation admits separable solutions in radial and angular variables. The angular equation reduces to a generalized spheroidal harmonic form, while the radial equation can be expressed in terms of the double confluent Heun function. By analyzing the asymptotic behavior of the radial solution, we establish the existence of bound-state scalar clouds characterized by a discrete mass spectrum. We further outline how the (quasi)bound spectrum can be extracted using the continued-fraction method of Vieira–Bezerra–Kokkotas (VBK).

1 Introduction

Black holes immersed in external fields provide a fertile ground for exploring the dynamics of classical gravity, quantum field theory in curved spacetime, and astrophysical phenomena. Among such interactions, the behavior of scalar fields around rotating black holes has been a topic of sustained interest due to the superradiant scattering process, where energy and angular momentum can be extracted from the rotation of the black hole [1–3]. At the threshold of superradiance, specific scalar modes may form long-lived, nonradiating configurations known as scalar clouds–bound states that signify the onset of scalar hair and break the standard no-hair paradigm [4,5].

These stationary bound states have been thoroughly investigated in the Kerr and Kerr–Newman families of spacetimes [6–8], and in alternative black hole geometries such as those arising in modified gravity theories [9–12]. Their significance extends to a variety of contexts, from the search for light bosonic fields in the string axiverse [13,14] to tests of strong-field gravity through gravitational waves [15,16]. Additionally, analogous configurations have been proposed in analogue gravity systems such as acoustic black holes [17,18].

When considering more realistic astrophysical scenarios, however, the role of magnetic fields cannot be ignored [19]. Observational and theoretical studies suggest that black holes may reside in environments threaded by magnetic fields originating from accretion disks, jets, or interstellar plasma [20–22]. The influence of such external fields on black hole dynamics and field perturbations has sparked a series of investigations, notably on scalar instabilities and modified quasi-bound states [23–26]. In this context, the Melvin–Kerr spacetime, describing a rotating black hole embedded in a cylindrical magnetic universe, offers a compelling testbed. This class of solutions is generated via Harrison transformations applied to the Kerr metric and constitutes an exact solution to the coupled Einstein–Maxwell equations [20,21]. Shadows and gravitational lensing in magnetized black holes have been investigated in [27,28], whereas the quasinormal modes are discussed in [29]. Several extensions have further explored its generalizations involving NUT charges, electric charges, and holographic interpretations [30–35].

Despite the growing literature on magnetized black hole spacetimes, the existence and structure of stationary scalar clouds in Melvin–Kerr backgrounds remain largely unexplored. For instance, the investigation in [25] addressed scalar clouds specifically around magnetized Reissner–Nordstrom black holes. In a rotating spacetime, the introduction of a magnetic field modifies both the geometry and the gauge interaction experienced by a charged scalar field, leading to a more intricate dynamics and richer phenomenology [22,33,34,36–38]. In particular, the interplay between gravitational attraction, centrifugal barriers, and magnetic

[a] e-mail: haryanto.siahaan@unpar.ac.id (corresponding author)

Published online: 15 September 2025

coupling reshapes the conditions for the formation of bound states.

In this paper, we study the dynamics of a massive, charged scalar field in the Melvin–Kerr background under the assumption of a weak magnetic field ($bM \ll 1$). We demonstrate that the Klein–Gordon equation in this background is separable, yielding an angular equation that generalizes spheroidal harmonics and a radial equation characterized by effective potentials that include magnetic corrections. The resulting radial equation admits solutions in terms of special functions, including the double confluent Heun function–a structure that naturally arises in complex gravitational systems with irregular singularities [39–41].

Our goal is to establish the existence of scalar clouds in this setting, i.e. regular stationary solutions that correspond to discrete values of the scalar mass μ, synchronized with the horizon angular velocity via the superradiant threshold $\omega = m\Omega_H$. By analyzing the asymptotic behavior of the radial wave function near the horizon and at spatial infinity, we derive a quantization condition that characterizes the bound-state nature of the solution. To ensure both boundary conditions are consistently implemented, we also outline the Vieira–Bezerra–Kokkotas (VBK) continued-fraction method [42–44], which provides a robust framework for extracting (quasi)bound-state spectra from double confluent Heun equations. In this way we extend earlier studies of scalar clouds around Kerr [4,6], Kerr–Newman [5,7], and other rotating black hole backgrounds, and highlight how the presence of an external magnetic field modifies the conditions for cloud formation compared with the unmagnetized case.

The results presented in this work extend previous investigations on scalar clouds in Kerr [4,6], Kerr–Newman [5,7], and various modified black hole spacetimes [45,46], by introducing a magnetic field as a nontrivial background element. Our analysis also intersects with ongoing research on scalar hair, quasinormal modes, and nonlinear extensions [6,8,47], thereby contributing to a more comprehensive understanding of scalar field dynamics in physically motivated black hole backgrounds. For analytical simplicity, we adopt the method employed in [4], where the black hole is assumed to be in an extremal state. Remarkably, the extremal condition for both Kerr and Melvin–Kerr black holes coincides, characterized by the relation $M = a$, with M denoting the black hole mass and a the spin parameter.

The structure of this paper is as follows. In Sect. 2, we briefly review the Melvin–Kerr solution. Section 3 presents the Klein–Gordon equation for a massive charged scalar field and its separation into radial and angular parts. In Sect. 4, we establish the conditions for scalar cloud formation, analyze the resonance mass spectrum, and discuss the role of the magnetic field. Section 5 summarizes our findings and outlines possible extensions. For completeness, the appendices provide the mapping of the radial equation to the double confluent Heun form and the details of the Vieira–Bezerra–Kokkotas (VBK) continued-fraction method used to implement the boundary conditions. Throughout this work, we employ natural units where $c = G_N = \hbar = 1$.

2 Review of the Melvin–Kerr spacetime

The Melvin–Kerr spacetime describes a rotating black hole immersed in an external, axisymmetric magnetic field. This solution generalizes the standard Kerr black hole by incorporating a uniform magnetic field through a Harrison-type transformation in the Einstein–Maxwell theory [20]. The resulting geometry remains stationary and axisymmetric but features a nontrivial interplay between rotation and electromagnetic fields. In this section, we review the structure of the Melvin–Kerr metric and the associated electromagnetic field, focusing on the form of the line element, metric functions, and vector potential components. These expressions form the foundation for the analysis of charged scalar field dynamics that follows in subsequent sections.

The line element for this geometry is given by

$$\begin{aligned} ds^2 &= \frac{\Delta \sin^2\theta}{f} dt^2 - \frac{e^{2\gamma}}{f}\left(\frac{dr^2}{\Delta} + d\theta^2\right) \\ &\quad - f\,(\omega dt - d\phi)^2\,, \end{aligned} \tag{2.1}$$

where

$$\Delta = r^2 - 2Mr + a^2, \tag{2.2}$$

$$e^{2\gamma} = \sin^2\theta\left(\Delta a^2\cos^2\theta + r(r^3 + a^2 r + 2a^2 M)\right), \tag{2.3}$$

$$f = \frac{e^{2\gamma}}{c_0 + c_2 b^2 + c_4 b^4}, \tag{2.4}$$

and

$$\omega = -\frac{2aM\sin^2\theta}{e^{2\gamma}}\left[\left(d_0 + d_2\cos^2\theta + d_4\cos^4\theta\right)b^4 - r\right]. \tag{2.5}$$

The coefficient functions appearing in f and ω are given by

$$c_0 = r^2 + a^2\cos^2\theta, \tag{2.6}$$

$$\begin{aligned} c_2 &= 2a^2\Delta\cos^4\theta + 2(r^4 + 4a^2Mr - a^4)\cos^2\theta \\ &\quad - 2r(r^3 + a^2 r + 2a^2 M), \end{aligned} \tag{2.7}$$

$$\begin{aligned} c_4 &= a^2\Delta^2\cos^6\theta \\ &\quad + \left(4a^4M^2 - 2a^6 + 12a^4Mr - 3a^4r^2 - 24a^2M^2r^2\right. \\ &\quad \left. + 12a^2Mr^3 + r^6\right)\cos^4\theta \\ &\quad + \left(a^6 + 8a^4M^2 - 12a^4Mr + 36a^2M^2r^2 - 12a^2Mr^3\right. \\ &\quad \left. - 3a^2r^4 - 2r^6\right)\cos^2\theta + \left(2a^2M + a^2r + r^3\right)^2, \end{aligned} \tag{2.8}$$

$$d_0 = (2a^2M + a^2r + r^3)(a^2 - 3r^2), \tag{2.9}$$

$$d_2 = 6\Delta(a^2M - a^2r - r^3), \tag{2.10}$$

$$d_4 = (2a^2M - 3a^2r + r^3)\Delta. \tag{2.11}$$

This geometry incorporates three fundamental physical parameters, i.e. the mass M, the rotational parameter a, and the magnetic field parameter b, representing the strength of an external, asymptotically uniform magnetic field aligned with the axis of symmetry. The inclusion of b profoundly affects the structure of the spacetime. It modifies the gravitational potential f and the frame-dragging effect encoded in ω. For $b = 0$, the geometry reduces smoothly to the standard Kerr spacetime, while for non-zero b, it asymptotically approaches a magnetized universe akin to the Melvin solution. Thus, the Melvin–Kerr solution may be regarded as a non-asymptotically flat extension of the Kerr black hole, offering a framework to model the influence of external magnetic fields on rotating compact objects, which is particularly relevant in astrophysical environments such as those found near accretion disks or active galactic nuclei.

The accompanying vector potential $A_\mu dx^\mu = A_t\, dt + A_\phi\, d\phi$ in the Melvin–Kerr background arises naturally from the solution-generating procedure that embeds the Kerr geometry in an external magnetic field. The components of the vector potential are given by

$$A_t = \frac{2bM\left(k_0 + k_2\cos^2\theta + k_4\cos^4\theta + k_6\cos^6\theta\right)}{a\,\Xi}, \tag{2.12}$$

$$A_\phi = \frac{b\left(l_0 + l_2\cos^2\theta + l_4\cos^4\theta + l_6\cos^6\theta\right)}{\Xi}, \tag{2.13}$$

where the coefficient functions are expressed as follows

$$\begin{aligned} k_0 = {} & \left(2a^2b^2M + a^2b^2r + b^2r^3 - r\right)\left(a^4b^2 + 4a^2b^2M^2\right. \\ & \left. +2a^2b^2Mr - 3a^2b^2r^2 + 2b^2Mr^3 - a^2 - 2Mr\right), \end{aligned} \tag{2.14}$$

$$\begin{aligned} k_2 = {} & 16M^3a^4b^4 + 72M^3a^2b^4r^2 - 36M^2a^4b^4r \\ & - 24M^2a^2b^4r^3 + 6Ma^6b^4 + 24Ma^4b^4r^2 \\ & + 6Ma^2b^4r^4 - 4Mb^4r^6 - 7a^6b^4r - 10a^4b^4r^3 \\ & - 3a^2b^4r^5 + 16M^2a^2b^2r - 10Ma^4b^2 \\ & - 12Ma^2b^2r^2 + 4Mb^2r^4 + 8a^4b^2r + 8a^2b^2r^3 \\ & + 2Ma^2 - a^2r, \end{aligned} \tag{2.15}$$

$$\begin{aligned} k_4 = {} & -b^2\left(16Ma^4b^2r^2 - 8M^3a^4b^2 + 48M^3a^2b^2r^2\right. \\ & - 32M^2a^4b^2r - 24M^2a^2b^2r^3 + 8Ma^6b^2 \\ & + 14Ma^2b^2r^4 - 2Mb^2r^6 - 3a^6b^2r - 10a^4b^2r^3 \\ & \left. - 7a^2b^2r^5 + 8M^2a^2r \right. \\ & \left. -2Ma^4 - 6Ma^2r^2 - 2a^4r + 2r^3a^2\right), \end{aligned} \tag{2.16}$$

$$k_6 = a^2b^4r\Delta\left(2\,Mr - 4\,M^2 + 3\,a^2 - r^2\right), \tag{2.17}$$

and

$$l_0 = \left(2a^2M + a^2r + r^3\right)\left(2a^2b^2M + a^2b^2r + b^2r^3 - r\right), \tag{2.18}$$

$$\begin{aligned} l_2 = {} & a^6b^2 + 8a^4b^2M^2 - 12a^4b^2Mr + 36a^2b^2M^2r^2 \\ & - 12a^2b^2Mr^3 - 3a^2b^2r^4 - 2b^2r^6 - a^4 + 4a^2Mr + r^4, \end{aligned} \tag{2.19}$$

$$\begin{aligned} l_4 = {} & 4a^4b^2M^2 - 2a^6b^2 + 12a^4b^2Mr \\ & - 3a^4b^2r^2 - 24a^2b^2M^2r^2 \\ & + 12a^2b^2Mr^3 + b^2r^6 + a^4 - 2a^2Mr + a^2r^2, \end{aligned} \tag{2.20}$$

$$l_6 = a^2b^2\Delta_r^2, \tag{2.21}$$

where the denominator Ξ appearing in both components is given by

$$\begin{aligned} \Xi = {} & \left(2a^2b^2M + a^2b^2r + b^2r^3 - r\right)^2 + k_2\cos^2\theta \\ & + k_4\cos^4\theta + k_6\cos^6\theta. \end{aligned} \tag{2.22}$$

These fields obey the equations of motion in Einstein-Maxwell theory, i.e.

$$R_{\mu\nu} = 2F_{\mu\alpha}F^{\alpha}_{\nu} - \frac{1}{2}g_{\mu\nu}F_{\alpha\beta}F^{\alpha\beta}, \tag{2.23}$$

and the source-free conditions

$$\nabla_\mu F^{\mu\nu} = 0. \tag{2.24}$$

This solution is generated by applying the Ernst magnetization procedure to the Kerr metric, serving as the seed solution [20]. The Ernst magnetization is a special case of the more general Harrison transformation, a class of powerful solution-generating techniques in the Einstein–Maxwell theory. These transformations enable the construction of new exact solutions from known stationary and axisymmetric spacetimes by incorporating additional physical effects. The Harrison transformation acts on the Ernst potentials, which are complex scalar functions encoding both the gravitational and electromagnetic structures of the spacetime. These potentials–denoted by $\mathcal{E}$ for the gravitational field and Φ for the electromagnetic field–satisfy a coupled system of nonlinear partial differential equations known as the Ernst equations.

The process of Ernst magnetization can be summarized as follows. Given a seed solution characterized by a pair of Ernst potentials $(\mathcal{E}_0, \Phi_0)$, the Harrison transformation yields

a magnetized configuration through the transformation:

$$\mathcal{E} \to \frac{\mathcal{E}_0}{|\Lambda|^2}, \quad \Phi \to \frac{\Phi_0 + \frac{1}{2}b\mathcal{E}_0}{|\Lambda|^2}, \tag{2.25}$$

where the function Λ is given by

$$\Lambda = 1 + b\Phi_0 + \frac{1}{4}b^2\mathcal{E}_0, \tag{2.26}$$

and $b \in \mathbb{R}$ is a real parameter quantifying the strength of the external magnetic field. This transformation not only alters the spacetime metric but also modifies the electromagnetic vector potential, leading to a geometry that is no longer asymptotically flat but asymptotically Melvin. This approach has been employed to construct a wide range of magnetized black hole solutions, including Melvin–Schwarzschild, Melvin–Reissner–Nordström, Melvin–Kerr, and Melvin–Kerr–Newman spacetimes [20,33,34].

3 Massive charged scalar fields in Melvin–Kerr background

With the Melvin–Kerr geometry and its electromagnetic field structure established, we now turn our attention to the dynamics of a massive, charged test scalar field propagating in this background. This analysis is governed by the minimally coupled Klein–Gordon (KG) equation, which incorporates both gravitational and electromagnetic interactions. The stationary and axisymmetric nature of the spacetime allows for a separation of variables in the scalar field, facilitating a decomposition into radial and angular parts. However, due to the presence of the magnetic field parameter and the complexity of the background, obtaining separable equations requires a judicious approximation scheme. In the following, we derive the approximate form of the KG equation in the weak-field limit $bM \ll 1$, identify the separable structure of the field equations, and investigate the resulting angular and radial dynamics that underpin the formation of bound scalar clouds around magnetized Kerr black holes. This limit is motivated by astrophysical considerations, since regions in the universe with significantly strong magnetic fields are not known to exist.

Let us now consider the propagation of a massive, charged scalar field in the Melvin–Kerr spacetime by analyzing the covariant KG equation minimally coupled to the background electromagnetic field. The equation governing the dynamics of such a test scalar field is given by

$$\left\{\left(\nabla_\mu - iqA_\mu\right)\left(\nabla^\mu - iqA^\mu\right) - \mu^2\right\}\Phi = 0, \tag{3.1}$$

where μ and q denote the mass and charge of the scalar field, respectively, and A_μ is the electromagnetic potential derived in the previous section. Owing to the spacetime's stationarity and axisymmetry, the KG equation admits a separable ansatz for the scalar field

$$\Phi(t, r, \theta, \phi) = \sum_{l,m} e^{i(m\phi - \omega t)} R_{lm}(r)\, S_{lm}(\theta), \tag{3.2}$$

where ω is the conserved frequency associated with time translation invariance, and m is the azimuthal quantum number due to axial symmetry.

Substituting this ansatz into the KG equation leads to a coupled partial differential equation that contains radial and angular derivatives. Rearranging the terms and factoring out the radial and angular dependencies, the equation takes the form

$$\begin{aligned}&\frac{1}{R_{lm}}\frac{d}{dr}\left(\Delta\frac{dR_{lm}}{dr}\right) + \frac{1}{\sin\theta\, S_{lm}}\frac{d}{d\theta}\left(\sin\theta\frac{dS_{lm}}{d\theta}\right)\\ &+\Big[f_{(\mu^2)}\mu^2 + f_{(\omega^2)}\omega^2 + f_{(\omega)}\omega + f_{(m^2)}m^2\\ &+f_{(m)}m + f_{(0)}\Big] = 0.\end{aligned} \tag{3.3}$$

Here, the functions $f_{(*)}$ encode the nontrivial couplings between the scalar field and the geometry, as well as the electromagnetic background. These functions depend explicitly on r, θ, and the spacetime parameters, and are provided in detail in the appendix A. The full KG equation for a massive, charged test scalar field propagating in the Melvin–Kerr spacetime exhibits a highly intricate structure due to the combined effects of spacetime curvature, rotation, and the background electromagnetic field. In its general form, demonstrating separability of the equation into radial and angular parts is far from trivial. The nontrivial coupling between the scalar field parameters (μ, q) and the black hole's physical properties (M, a) in the presence of an external magnetic field (b) leads to cross-terms that obstruct a straightforward factorization.

To make analytical progress, we invoke a physically reasonable assumption that the magnetic field is relatively weak compared to the characteristic gravitational scale, i.e., $bM \ll 1$. Under this approximation, magnetic interaction terms can be expanded and truncated at leading order in b. This simplification enables a manageable decomposition of the KG equation, where the coefficient functions $f_{(*)}$ reduce to expressions that are either independent of b, or linear in b and hence tractable analytically. In such consideration, the approximated forms of the coefficient functions under this weak-field limit are as follows

$$f_{(\mu^2)} \approx -r^2 - a^2\cos^2\theta\,, \tag{3.4}$$

$$f_{(\omega^2)} \approx a^2\cos^2\theta + \frac{r(2a^2M + a^2r + r^3)}{\Delta}\,, \tag{3.5}$$

$$f_{(\omega)} \approx -\frac{4aMmr}{\Delta}$$

$$+ 8M^2qb\left[a\cos^2\theta + \frac{r(2a^2M + a^2r + r^3)}{a\Delta}\right], \tag{3.6}$$

$$f_{(m^2)} \approx \frac{a^2}{\Delta} - \frac{1}{\sin^2\theta}, \tag{3.7}$$

$$f_{(m)} \approx -2bq\left[a^2\cos^2\theta + \frac{r(8M^3 + a^2r - 2Mr^2 + r^3)}{\Delta}\right], \tag{3.8}$$

$$f_{(0)} \approx 0. \tag{3.9}$$

These simplified expressions play an important role in facilitating the separation of the KG equation into radial and angular components, thereby allowing further analytical treatment.

The application of the small-bM approximation to the KG equation allows for a complete separation of variables, yielding two coupled ordinary differential equations: one in the radial coordinate r, and the other in the angular coordinate θ. The radial equation governs the dynamics of the scalar field along the black hole's radial direction and takes the following form

$$\frac{d}{dr}\left(\Delta\frac{dR_{lm}}{dr}\right) + \left[\frac{H^2}{\Delta} + 2ma\omega - \mu^2(r^2 + a^2) + \frac{2bqrZ_r}{a\Delta} - K_{lm}\right]R_{lm} = 0, \tag{3.10}$$

where $H = (r^2 + a^2)\omega - am$ and

$$Z_r = 4M^2\omega(2Ma^2 + a^2r + r^3) - am(8M^3 - 2Mr^2 + a^2r + r^3) \tag{3.11}$$

which captures the interplay between the black hole's angular momentum, the external magnetic field, and the scalar field.

Within the small-bM regime, the influence of the magnetic field on the radial dynamics is entirely captured by the term proportional to bqZ_r. This contribution modifies the effective potential and illustrates how the scalar field couples to the background electromagnetic field. In the absence of this term, the equation reduces to the standard Kerr case, as discussed in [4]. Furthermore, the presence of the $1/\Delta$ structure highlights that the behavior of solutions near the event horizon, i.e. $\Delta \to 0$, is highly sensitive to both the field parameters and the background geometry. Consequently, this setup provides a useful model for studying the dynamics of a charged massive scalar field around a magnetized black hole, where the influence of the external magnetic field is most significant near the horizon.

On the other hand, the angular part governs the latitudinal variation of the scalar field and generalizes the familiar spheroidal wave equation by introducing additional couplings due to the mass μ and charge q of the scalar field, as well as the magnetic field b

$$\frac{1}{\sin\theta}\frac{d}{d\theta}\left(\sin\theta\frac{dS_{lm}}{d\theta}\right) + \Big\{K_{lm} + a^2(\mu^2 - \omega^2) - \left[a^2(\mu^2 - \omega^2) - 2aqb(4M^2\omega - am)\right]\cos^2\theta - \frac{m^2}{\sin^2\theta}\Big\}S_{lm} = 0. \tag{3.12}$$

This angular equation reduces to the usual spheroidal harmonic equation for Kerr case in the limit $b \to 0$, and the separation constant K_{lm} plays the role of a generalized eigenvalue encoding the angular momentum and field interactions. The term proportional to bq introduces an additional angular dependence not present in the Kerr or Kerr–Newman scenarios, reflecting the coupling between the scalar field and the external magnetic field. This interaction affects the angular eigenfunctions $S_{lm}(\theta)$, which remain regular on the interval $\theta \in [0, \pi]$.

By introducing the substitution $x = \cos\theta$, the angular equation (3.12) can be recast into the standard form of a prolate spheroidal wave equation [41], which is well-known in mathematical physics for describing angular functions in oblate and prolate spheroidal coordinate systems. The resulting equation reads

$$\frac{d}{dx}\left[\left(1 - x^2\right)\frac{dS_{lm}}{dx}\right] + \left(\lambda_{lm} - c^2x^2 - \frac{m^2}{1 - x^2}\right)S_{lm} = 0, \tag{3.13}$$

where the effective spheroidicity parameter c^2 and the angular eigenvalue λ_{lm} are defined as

$$c^2 = a^2\left(\mu^2 - \omega^2\right) - 2aqb\left(4M^2\omega - am\right), \tag{3.14}$$

and

$$\lambda_{lm} = K_{lm} + a^2\left(\mu^2 - \omega^2\right). \tag{3.15}$$

The equation above governs the angular behavior of the charged scalar field in the magnetized Kerr background, where the effect of the external magnetic field enters through the additional term in c^2 proportional to bq. In the limit where $c = 0$, i.e. both a and b vanish, the equation reduces to the standard associated Legendre differential equation, and its solutions become the associated Legendre polynomials $P_l^m(x)$.

For small but non-zero values of c^2, which is the case under the weak magnetic field approximation $bM \ll 1$, the spheroidal term c^2x^2 can be treated as a perturbation to the Legendre equation. In this regime, one can approximate the angular eigenvalue λ_{lm} to first order in c^2 using perturbation theory [41,48]

$$\lambda_{lm} \cong l(l + 1) + \frac{2c^2\left[m^2 + \frac{1}{2} - l(l + 1)\right]}{(2l + 3)(2l - 1)}. \tag{3.16}$$

This expression reveals how the angular eigenvalue deviates from the unperturbed Legendre case due to the combined effects of field mass, frequency, and magnetic coupling. The perturbative form of λ_{lm} is instrumental for analytically estimating the spectrum of bound scalar field configurations, particularly when determining the existence and properties of stationary scalar clouds in the next section.

Now let us turn our attention to the radial part of the KG equation. To facilitate the analysis and handle the coordinate singularity at the horizon, we introduce the tortoise coordinate y, defined via the relation

$$\frac{dy}{dr} = \frac{r^2 + a^2}{\Delta}, \tag{3.17}$$

which maps the near-horizon region $r \to r_+$ to $y \to -\infty$, and spatial infinity $r \to \infty$ to $y \to +\infty$. This coordinate transformation allows a clearer interpretation of the wave behavior near the horizon and at infinity, particularly when imposing physically relevant boundary conditions. In addition to the tortoise coordinate, we redefine the radial function as $Y_{lm} = \sqrt{r^2 + a^2}\, R_{lm}$, which absorbs some of the background geometry's radial structure and simplifies the form of the differential equation. In this approach, the radial equation (3.10) can be written in a compact and self-adjoint form

$$\Delta \frac{d}{dr}\left(\Delta \frac{d}{dr}\left(\frac{Y_{lm}}{\sqrt{r^2 + a^2}}\right)\right) + \Delta K \frac{Y_{lm}}{\sqrt{r^2 + a^2}} = 0, \tag{3.18}$$

where the radial potential can be expressed as

$$K = \frac{H^2}{\Delta} + 2ma\omega - \mu^2(r^2 + a^2) + \frac{2bqrZ_r}{a\Delta} - K_{lm}. \tag{3.19}$$

After some algebraic manipulation, the radial equation can be written more transparently as

$$\frac{d^2 Y_{lm}}{dy^2} + V_{\text{eff}} Y_{lm} = 0, \tag{3.20}$$

where

$$V_{\text{eff}} = \frac{\Delta}{(r^2 + a^2)^4} \times \left\{(r^2 + a^2)^2 K - a^2(r^2 + a^2) + 2rM(2a^2 - r^2)\right\} \tag{3.21}$$

which now clearly resembles a one-dimensional wave equation with an effective potential depending on both the geometry and the scalar field parameters. This effective potential is illustrated in Fig. 1, showing the influence of the external magnetic field on the structure of the potential barrier and the conditions required for the existence of bound states.

From Fig. 1, we observe how the magnetic field modifies the potential barrier structure. Therefore, it plays a significant role in determining whether bound-state solutions, such as stationary scalar clouds, can exist around the magnetized

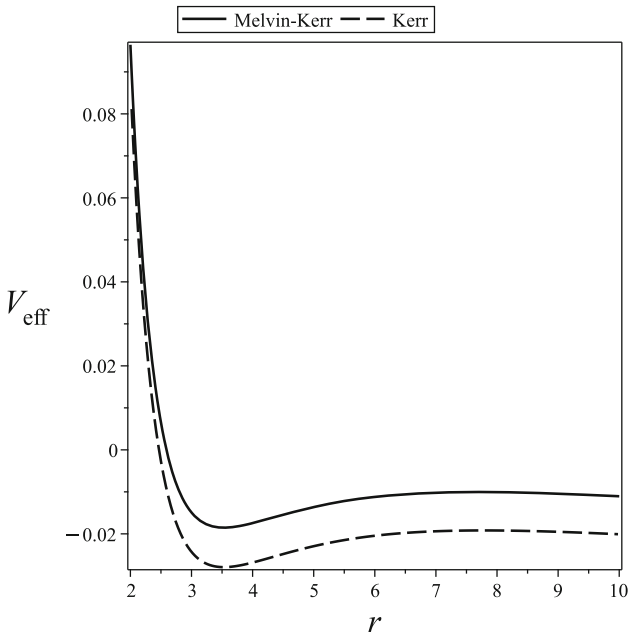

Fig. 1 Effective potential $V_{\text{eff}}(r)$ for the radial part of the KG equation in the Melvin–Kerr black hole background. The solid curve corresponds to the Melvin–Kerr case with $bM = 0.01$ and scalar charge $qM = 0.1$, while the dashed curve shows the unmagnetized case or Kerr. Other parameters are fixed as $a = 0.3M, \omega M = 0.4, \mu M = 0.45, m = 1$, and $l = 1$. The presence of the external magnetic field modifies the shape and depth of the potential well, which has significance in supporting stationary scalar configurations

Kerr black hole. To fully characterize such solutions, it is important to examine the asymptotic behavior of the radial equation in two key regions: near the event horizon and at spatial infinity. These asymptotic limits dictate the boundary conditions required for the existence of regular, localized scalar field configurations.

Near the event horizon, $r \to r_+$, the radial equation simplifies considerably. In this limit, the potential behaves as a constant, and the radial wave equation reduces to a Schrödinger-like form with an effective frequency-dependent term

$$\frac{d^2 Y_{lm}}{dy^2} + \left[(\omega - \omega_c)^2 + \frac{8bM^2 q}{a}(\omega - \omega_c)\right] Y_{lm} = 0, \tag{3.22}$$

where the critical frequency ω_c is defined as

$$\omega_c = \frac{ma}{2Mr_+}. \tag{3.23}$$

This result implies that the scalar field behaves as a purely ingoing wave at the horizon, and the physical solution must satisfy the condition

$$R_{lm} \sim e^{-ik_+ y}, \tag{3.24}$$

where the effective horizon momentum is given by

$$k_+ = \left[(\omega-\omega_c)^2 + \frac{8bM^2q}{a}(\omega-\omega_c)\right]^{1/2}. \tag{3.25}$$

This ingoing behavior is required to preserve the causal structure of the spacetime and ensure that no outgoing flux escapes from within the event horizon.

On the other hand, in the asymptotic region $r \to \infty$, the mass term μ^2 dominates over the potential, and the radial equation reduces to the simplified form

$$\frac{d^2Y_{lm}}{dy^2} + \left[\omega^2 - \mu^2 - \frac{2qb\left(am - 4M^2\omega\right)}{a}\right] Y_{lm} = 0, \tag{3.26}$$

which yields the asymptotic behavior

$$R_{lm} \sim \frac{1}{r}\exp\left\{i\left[\omega^2 - \mu^2 - \frac{2qb(am-4M^2\omega)}{a}\right]^{1/2} y\right\}. \tag{3.27}$$

Imposing the condition

$$\omega^2 - \mu^2 - \frac{2qb(am-4M^2\omega)}{a} > 0, \tag{3.28}$$

ensures the asymptotic solution (3.27) describes an exponentially decaying field at spatial infinity, a necessary condition for the existence of bound-state configurations. This condition will be considered in the next section, where we demonstrate the existence of scalar clouds.

4 Bound-state scalar clouds in Melvin–Kerr geometry

Here we demonstrate that, similarly to the scenario of scalar clouds around extremal Kerr black holes discussed in [4], stationary bound states also exist in the presence of an external magnetic field under the superradiant condition $\omega = \omega_c$. To proceed analytically, we define a new dimensionless radial coordinate that simplifies the near-horizon expansion and captures the asymptotic behavior of the radial equation

$$x = \frac{r-M}{M}, \tag{4.1}$$

where M is the mass of the black hole. This rescaling sets the event horizon at $x = 0$, and transforms the radial equation into a generalized second-order ordinary differential equation of the form

$$x^2\frac{d^2R}{dx^2} + 2x\frac{dR}{dx} + \left(h_2x^2 + h_1x + h_0 + \frac{h_{-1}}{x}\right)R = 0, \tag{4.2}$$

with the coefficients

$$h_2 = 2bqM^2m - \mu^2M^2 + \frac{m^2}{4}, \qquad h_1 = 12bqM^2m - 2\mu^2M^2 + m^2, \tag{4.3}$$

$$h_0 = 26bqmM^2 - 2\mu^2M^2 + 2m^2 - K_{lm}, \qquad h_{-1} = 16M^2bqm. \tag{4.4}$$

Equation (4.2) belongs to the class of double confluent Heun equations (dCHE), characterized by two irregular singular points at $x = 0$ and $x = \infty$. Its correspondence with the canonical form of the dCHE, as presented in Ronveaux's book [39], is outlined in Appendix B. To determine the (quasi)bound-state spectrum, we employ the Vieira–Bezerra–Kokkotas (VBK) method [42–44,49], which incorporates the horizon-ingoing and infinity-decaying boundary conditions into a single continued-fraction equation for ω, constructed from the local series representation of the dCHE solution to Eq. (4.2). The algorithmic steps, including the reduction of recurrence relations and the resulting characteristic equation, are detailed in Appendix B.

As an alternative approach to establishing the existence of scalar clouds, we consider the far-region limit of the radial equation. This limit enables us to extract analytic features of the solution and, in particular, identify the quantization conditions responsible for the emergence of scalar cloud configurations. In the asymptotic region, where $x \gg 1$, terms containing inverse powers of x can be neglected. Under this approximation, the radial equation simplifies to a second-order linear differential equation of the form

$$x^2\frac{d^2R_{\rm far}}{dx^2} + 2x\frac{dR_{\rm far}}{dx} + \left(h_2x^2 + h_1x + h_0\right)R_{\rm far} = 0. \tag{4.5}$$

This reduced equation closely resembles the radial equation for a massive scalar field in the extremal Kerr geometry, as discussed in [4], with the crucial difference that here the external magnetic field introduces additional coupling through the coefficients h_2, h_1, and h_0. Remarkably, the equation above can be mapped to a standard Whittaker equation by introducing the substitutions

$$\tilde{R}(z) \equiv xR_{\rm far}(x), \quad \text{with} \quad x = \frac{z}{\sqrt{(4\mu^2-8bqm)M^2-m^2}}, \tag{4.6}$$

where the denominator defines an effective inverse length scale that encapsulates both the mass of the scalar field and the strength of its magnetic coupling.

Substituting this ansatz into the far-region radial equation yields the Whittaker differential equation

$$\frac{d^2\tilde{R}}{dz^2} + \left(-\frac{1}{4} + \frac{\kappa}{z} + \frac{1-4\beta^2}{4z^2}\right)\tilde{R} = 0, \tag{4.7}$$

where the parameters κ and β are defined by

$$\kappa = \frac{m^2 - 2M^2\left(\mu^2 - 6bqm\right)}{\sqrt{\left(4\mu^2 - 8bqm\right)M^2 - m^2}}, \tag{4.8}$$

$$\beta^2 = \frac{1}{4} + K_{lm} - 2m^2 + 2M^2\left(\mu^2 - 13bqm\right). \tag{4.9}$$

The general solution to the Whittaker equation is given by a linear combination of confluent hypergeometric functions $\mathcal{M}$ and $\mathcal{U}$, such that

$$R_{\rm far}(z) = C_1 z^{\beta+1/2} e^{-z/2} \mathcal{M}\left(\beta - \kappa + \frac{1}{2}, 1 + 2\beta, z\right) + C_2 z^{\beta+1/2} e^{-z/2} \mathcal{U}\left(\beta - \kappa + \frac{1}{2}, 1 + 2\beta, z\right), \tag{4.10}$$

where C_1 and C_2 are integration constants. The confluent hypergeometric function $\mathcal{U}$ decays exponentially as $z \to \infty$, and thus satisfies the requirement for a bound state. However, the $\mathcal{M}$ function generally grows exponentially for large z, as seen in the asymptotic form

$$\mathcal{M}(\alpha, \beta, z) \sim \Gamma(\beta)\left[\frac{e^z z^{\alpha-\beta}}{\Gamma(\alpha)} + \frac{(-z)^{-\alpha}}{\Gamma(\beta - \alpha)}\right]. \tag{4.11}$$

To avoid the unphysical divergences at infinity, one must eliminate this growing contribution. This can be achieved either by setting $C_1 = 0$ or, more interestingly, by requiring that $\Gamma(\alpha) \to \infty$. The latter occurs if

$$\beta - \kappa + \frac{1}{2} = -n, \quad n \in \mathbb{N}_0, \tag{4.12}$$

which acts as a quantization condition for the existence of bound-state scalar modes. Each value of n corresponds to a specific discrete mode of the scalar field that is regular at the horizon and decays at spatial infinity.

Equation (4.12) thus plays the role of a Bohr-like condition for scalar clouds in magnetized Kerr spacetimes. It implies that only certain discrete combinations of black hole parameters (M, a), scalar field properties (μ, q, m), and magnetic field strength b allow the formation of such non-dissipative field configurations. This is consistent with earlier studies of stationary bound states in rotating geometries [4,6], and shows how magnetization enriches the parameter space for possible cloud formation.

Now, to ensure that the parameter κ defined in Eq. (4.8) remains positive–a requirement for the validity of the bound-state solution with decaying behavior at spatial infinity–the mass μ of the charged scalar field must lie within a specific range. This range ensures that the quantity under the square root in Eq. (4.8) is real and positive, and thus yields meaningful physical solutions. By direct analysis, one obtains the following band for the admissible values of μM

$$\frac{1}{2}\sqrt{m\left(m + 8M^2bq\right)} < \mu M < \sqrt{\frac{m\left(m + 12M^2bq\right)}{2}}. \tag{4.13}$$

It is evident from this inequality that modes with $m = 0$ are excluded, since they do not support a non-trivial bound state in the stationary case. This outcome is consistent with our previous assumption that the scalar field is stationary with angular frequency $\omega = \omega_c$, which necessitates a non-zero azimuthal quantum number m.

To further support the discrete nature of scalar clouds, let us verify the resonance condition derived in Eq. (4.12), using the expression for β and the approximate angular eigenvalue K_{lm} from Eqs. (3.15) and (3.16). Rather than explicitly presenting the cumbersome analytic expression, we numerically evaluate the mass spectrum for the fundamental modes with $l = 1$ and $m = 1$. We consider two scenarios, one without the magnetic field and scalar charge $(q = 0, b = 0)$, and one with small but non-zero values $(qM = 10^{-4}, bM = 10^{-5})$.

Table 1 The first four discrete mass values $M\mu_{\rm resonance}$ of the scalar field supporting bound-state solutions for $l = m = 1$. The left column corresponds to the Kerr background without magnetic or electric couplings, and the right column includes a weak external magnetic field $(bM = 10^{-5})$ and charge $(qM = 10^{-4})$

n	$M\mu_{\rm resonance}(q = 0, b = 0)$	$M\mu_{\rm resonance}(q \neq 0, b \neq 0)$
0	0.5256802790	0.5256802822
1	0.5101263130	0.5101263156
2	0.5052505930	0.5052505953
3	0.5031832280	0.5031832302

The numerical values in Table 1 demonstrate that the presence of an external magnetic field slightly shifts the resonant mass spectrum, confirming the subtle but non-negligible role of the bq coupling in shaping the structure of scalar clouds. Importantly, all mass values remain confined within the bounds specified in Eq. (4.13), validating the analytic estimate of the allowed mass range. Explicitly, for the chosen parameters, the admissible band reads

$$0.5000000020 < \mu M < 0.7071067852. \tag{4.14}$$

This confirms that the condition $\kappa > 0$ not only guarantees physically consistent bound states, but also constrains the mass parameter μ in a manner influenced by the scalar charge, magnetic field strength, and the mode number m, consistent with prior studies on scalar clouds around rotating black holes [4,7].

Quasi(bound) states are defined by the simultaneous imposition of two physical boundary conditions: (i) purely ingoing behavior at the event horizon and (ii) exponential decay at spatial infinity. In the rescaled coordinate $x = (r - M)/M$,

with the extremal horizon at $x = 0$, the tortoise relation $dy/dr = (r^2 + a^2)/\Delta$ gives $y \simeq -2M/x$ near the horizon ($a = M$). The ingoing condition is therefore

$$R_{\rm in}(x) \propto e^{-ik_+ y} \sim \exp\Big(\frac{i\,\eta_H(\omega)}{x}\Big), \tag{4.15}$$

where $\eta_H(\omega) = 2M\,k_+(\omega)$ and $k_+(\omega)$ is the effective horizon wave number including magnetic corrections (cf. Eq. (3.25)). By introducing the gauge $R = e^{\tau/x}u$ with $\tau = i\,\eta_H(\omega)$, the function $u(x)$ remains regular at $x = 0$, thereby enforcing the ingoing boundary condition. At spatial infinity, the radial solution behaves as

$$R_\infty(x) \sim \frac{1}{x}\exp\big(-M\,\kappa_\infty(\omega)\,x\big),$$
$$\kappa_\infty(\omega) = \sqrt{\mu^2 - \omega^2 - \tfrac{2qb}{a}(am - 4M^2\omega)}, \tag{4.16}$$

which decays exponentially whenever $\Re\,\kappa_\infty(\omega) > 0$.

The discrete spectrum follows by enforcing both conditions simultaneously. This is achieved by matching the horizon-ingoing and infinity-decaying solutions at an intermediate point $x_* > 0$ within their common domain of convergence. In practice, the matching is implemented through the Vieira–Bezerra–Kokkotas (VBK) continued-fraction scheme, applied to the local series of the double confluent Heun solution of Eq. (4.2). The resulting characteristic equation,

$$\mathcal{F}(\omega) := \mathcal{L}_{\rm in}(\omega; x_*) - \mathcal{L}_\infty(\omega; x_*) = 0, \tag{4.17}$$

yields the allowed (quasi)bound-state frequencies. Algorithmic details (series ansätze, recurrences, and continued fractions) are provided in Appendix B.

5 Discussions and conclusions

In this work, we have investigated stationary bound-state scalar configurations—scalar clouds—around magnetized Kerr black holes in the Einstein–Maxwell framework. By studying a charged, massive scalar field in the Melvin–Kerr geometry under the weak magnetic field approximation ($bM \ll 1$), we showed that the Klein–Gordon equation separates into radial and angular parts. The angular equation reduces to a generalized spheroidal harmonic form, while the radial equation belongs to the class of double confluent Heun equations (dCHE).

In the far-region limit, the radial equation reduces to a Whittaker form, allowing analytic treatment. By imposing regularity at the horizon and exponential decay at infinity, we derived a quantization condition that yields discrete bands of admissible scalar masses μ. These results establish the existence of stationary scalar clouds at the superradiant threshold, generalizing the well-known Kerr and Kerr–Newman cases to magnetized Kerr black holes. The analytic resonance bands highlight how the external magnetic field modifies both the effective potential and the cloud spectrum.

To address the boundary conditions more systematically, we outlined how the Vieira–Bezerra–Kokkotas (VBK) continued-fraction method can be adapted to the present dCHE structure. Although not carried out in detail here, the VBK scheme provides a natural framework to impose ingoing behavior at the horizon and exponential decay at infinity simultaneously, and thus to refine the spectrum beyond the far-region approximation. Implementing this procedure constitutes an important direction for future work.

Our findings extend earlier studies of scalar clouds around Kerr and Kerr–Newman black holes [4–7] to the magnetized Kerr geometry. They demonstrate that the interplay between rotation, charge, and external magnetic fields does not prevent cloud formation but instead enriches the spectrum of possible configurations. These results are relevant for astrophysical environments in which rotating black holes coexist with strong magnetic fields, such as active galactic nuclei or magnetized accretion flows [21].

Acknowledgements This work was supported by LPPM-UNPAR through the Penelitian Publikasi Internasional Bereputasi funding scheme. The author thanks the anonymous reviewer for his/her constructive comments and valuable suggestions, which have helped to improve the clarity and quality of this manuscript.

Data Availability Statement Data will be made available on reasonable request. [Author's comment: The datasets generated during and/or analysed during the current study are available from the corresponding author on reasonable request.]

Code Availability Statement Code/software will be made available on reasonable request. [Author's comment: The code/software generated during and/or analysed during the current study is available from the corresponding author on reasonable request.]

Funded by SCOAP[3].

A Full expressions of radial potential coefficients

In this appendix, we present the explicit forms of the coefficient functions $f_{(*)}$ appearing in the radial part of the Klein–Gordon equation (Eq. (3.3)). These functions encode the interplay of various physical parameters, including the

black hole mass M, spin parameter a, external magnetic field strength b, scalar charge q, and the scalar field parameters (μ, ω, m). The external magnetic field induces a rich angular dependence in the radial potential through powers of $\cos\theta$, leading to the decomposition of several coefficients into angular harmonics. The full expressions provided below facilitate both detailed analytical investigations and precise numerical implementations. Throughout this appendix, the radial coordinate r refers explicitly to the original Boyer–Lindquist coordinate.

$$
\begin{aligned}
f_{(\mu^2)} &= \Big\{\Big(4a^4Mr-2a^4r^2-4a^2M^2r^2+4a^2Mr^3-a^2r^4-a^6\Big)\cos^6\theta \\
&+\Big(2a^6+3a^4r^2-12a^2Mr^3-12a^4Mr-4a^4M^2-r^6 \\
&+24a^2M^2r^2\Big)\cos^4\theta+\Big(2r^6+12a^4Mr+3a^2r^4 \\
&-a^6-36a^2M^2r^2+12a^2Mr^3-8a^4M^2\Big)\cos^2\theta \\
&-4a^4M^2-4a^2Mr^3-4a^4Mr-r^6-2a^2r^4-a^4r^2\Big\}b^4 \\
&+\Big\{2r\left(2Ma^2+a^2r+r^3\right)-2a^2\Delta\cos^4\theta \\
&+2\left(a^4-r^4-2Ma^2r\right)\cos^2\theta\Big\}b^2 \\
&-a^2\cos^2\theta-r^2, \qquad \text{(A.1)}\\
f_{(\omega^2)} &= a^2\cos^2\theta+\frac{2a^2Mr+a^2r^2+r^4}{\Delta} \qquad \text{(A.2)}\\
f_{(\omega)} &= \frac{4}{a\Delta}\Big\{b^3\cos^4\theta\Big[3a^6qr-2a^6Mq+4a^4M^2qr \\
&-8a^4Mqr^2+2a^4qr^3+2a^2Mqr^4-a^2qr^5\Big] \\
&+b^4m\cos^4\theta\Big[2a^6M-3a^6r-4a^4M^2r+8a^4Mr^2 \\
&-2a^4r^3-2a^2Mr^4+a^2r^5\Big] \\
&+b^3\cos^2\theta\Big[6a^6qr-6a^6Mq+12a^4M^2qr \\
&-18a^4Mqr^2+12a^4qr^3-12a^2Mqr^4+6a^2qr^5\Big] \\
&+b^4m\cos^2\theta\Big[6a^6M-6a^6r-12a^4M^2r+18a^4Mr^2 \\
&-12a^4r^3+12a^2Mr^4-6a^2r^5\Big] \\
&+b^3\Big[6a^4Mqr^2-2a^6Mq-a^6qr+2a^4qr^3+3a^2qr^5\Big] \\
&+b^4m\Big[2a^6M+a^6r-6a^4Mr^2-2a^4r^3-3a^2r^5\Big] \\
&+b\Big[2a^4Mq\cos^2\theta-4a^2M^2qr\cos^2\theta+2a^2Mqr^2\cos^2\theta \\
&+4a^2M^2qr+2a^2Mqr^2+2Mqr^4\Big]-a^2mr\Big\}, \qquad \text{(A.3)}\\
f_{(m^2)} &= -\frac{1}{\Delta\sin^2\theta}\Big\{f^{(0)}_{(m^2)}+f^{(2)}_{(m^2)}\cos^2\theta+f^{(4)}_{(m^2)}\cos^4\theta \\
&+f^{(6)}_{(m^2)}\cos^6\theta+f^{(8)}_{(m^2)}\cos^8\theta+f^{(10)}_{(m^2)}\cos^{10}\theta\Big\}. \qquad \text{(A.4)}
\end{aligned}
$$

Each term $f^{(n)}_{(m^2)}$ is given below in the original expansion. These coefficients reflect the coupling of the azimuthal quantum number m to both the spacetime geometry and the external field via b, and they include multiple powers of r, a, and M.

$$
\begin{aligned}
f^{(0)}_{(m^2)} &= 32M^3a^6b^8r-16M^4a^6b^8-96M^3a^4b^8r^3+8M^2a^8b^8 \\
&+32M^2a^6b^8r^2-24M^2a^4b^8r^4-48M^2a^2b^8r^6+6Ma^8b^8r \\
&+16Ma^6b^8r^3+12Ma^4b^8r^5 \\
&-2Mb^8r^9+a^8b^8r^2+4a^6b^8r^4+6a^4b^8r^6+4a^2b^8r^8 \\
&+b^8r^{10}+32M^3a^4b^6r-16M^2a^6b^6+16M^2a^4b^6r^2 \\
&+32M^2a^2b^6r^4-16Ma^6b^6r-24Ma^4b^6r^3+8Mb^6r^7 \\
&-4a^6b^6r^2-12a^4b^6r^4-12a^2b^6r^6-4b^6r^8 \\
&+8M^2a^4b^4-48M^2a^2b^4r^2+12Ma^4b^4r-12Mb^4r^5 \\
&+6a^4b^4r^2+12a^2b^4r^4+6b^4r^6+8Mb^2r^3 \\
&-4a^2b^2r^2-4b^2r^4-2Mr+r^2, \qquad \text{(A.5)}\\
f^{(2)}_{(m^2)} &= 16M^4a^6b^8-576M^4a^4b^8r^2+240M^3a^6b^8r \\
&+384M^3a^4b^8r^3+144M^3a^2b^8r^5 \\
&+24M^2a^6b^8r^2+48M^2a^4b^8r^4+24M^2a^2b^8r^6 \\
&-32Ma^8b^8r-88Ma^6b^8r^3-72Ma^4b^8r^5 \\
&-8Ma^2b^8r^7+8Mb^8r^9+a^{10}b^8-10a^6b^8r^4-20a^4b^8r^6 \\
&-15a^2b^8r^8-4b^8r^{10}+32M^3a^4b^6r+288M^3a^2b^6r^3 \\
&-16M^2a^6b^6-288M^2a^4b^6r^2-272M^2a^2b^6r^4+72Ma^6b^6r \\
&+120Ma^4b^6r^3+24Ma^2b^6r^5-24Mb^6r^7-4a^8b^6 \\
&+24a^4b^6r^4+32a^2b^6r^6+12b^6r^8-48M^3a^2b^4r \\
&+16M^2a^4b^4+120M^2a^2b^4r^2-48Ma^4b^4r-24Ma^2b^4r^3 \\
&+24Mb^4r^5+6a^6b^4-18a^2b^4r^4-12b^4r^6+8Ma^2b^2r \\
&-8Mb^2r^3-4a^4b^2+4b^2r^4+a^2 \qquad \text{(A.6)}
\end{aligned}
$$

Also we have

$$
f_{(m)} = \frac{2bq}{\Delta\sin^2\theta}\Big\{f^{(0)}_{(m)}+f^{(2)}_{(m)}\cos^2\theta+f^{(4)}_{(m)}\cos^4\theta +f^{(6)}_{(m)}\cos^6\theta+f^{(8)}_{(m)}\cos^8\theta+f^{(10)}_{(m)}\cos^{10}\theta\Big\}. \qquad \text{(A.7)}
$$

The complete $f^{(n)}_{(m)}$ expressions similarly capture the interplay between charge q, magnetic field strength b, and the spacetime's rotation.

$$
\begin{aligned}
f^{(0)}_{(m)} &= -16M^4a^6b^6+32M^3a^6b^6r-96M^3a^4b^6r^3 \\
&+8M^2a^8b^6+32M^2a^6b^6r^2-24M^2a^4b^6r^4 \\
&-48M^2a^2b^6r^6+6Ma^8b^6r+16Ma^6b^6r^3 \\
&+12Ma^4b^6r^5-2Mb^6r^9+a^8b^6r^2+4a^6b^6r^4 \\
&+6a^4b^6r^6+4a^2b^6r^8+b^6r^{10}+16M^4a^4b^4 \\
&-48M^4a^2b^4r^2+32M^3a^4b^4r-16M^3a^2b^4r^3-24M^3b^4r^5 \\
&-12M^2a^6b^4+12M^2a^4b^4r^2+24M^2a^2b^4r^4 \\
&-12Ma^6b^4r-18Ma^4b^4r^3+6Mb^4r^7-3a^6b^4r^2-9a^4b^4r^4 \\
&-9a^2b^4r^6-3b^4r^8+4M^2a^4b^2-24M^2a^2b^2r^2+6Ma^4b^2r \\
&-6Mb^2r^5+3a^4b^2r^2+6a^2b^2r^4+3b^2r^6 \\
&-8M^3r+2Mr^3-a^2r^2-r^4, \qquad \text{(A.8)}\\
f^{(2)}_{(m)} &= 16M^4a^6b^6-576M^4a^4b^6r^2+240M^3a^6b^6r \\
&+384M^3a^4b^6r^3+144M^3a^2b^6r^5 \\
&+24M^2a^6b^6r^2+48M^2a^4b^6r^4+24M^2a^2b^6r^6
\end{aligned}
$$

$$
\begin{aligned}
&-32Ma^8b^6r-88Ma^6b^6r^3-72Ma^4b^6r^5-8Ma^2b^6r^7\\
&+8Mb^6r^9+a^{10}b^6-10a^6b^6r^4-20a^4b^6r^6-15a^2b^6r^8-4b^6r^{10}\\
&-96M^5a^2b^4r+32M^4a^4b^4+192M^4a^2b^4r^2+96M^4b^4r^4\\
&-32M^3a^4b^4r+136M^3a^2b^4r^3-24M^3b^4r^5-12M^2a^6b^4\\
&-216M^2a^4b^4r^2-204M^2a^2b^4r^4+54Ma^6b^4r\\
&+90Ma^4b^4r^3+18Ma^2b^4r^5-18Mb^4r^7-3a^8b^4\\
&+18a^4b^4r^4+24a^2b^4r^6+9b^4r^8-24M^3a^2b^2r\\
&+8M^2a^4b^2+60M^2a^2b^2r^2-24Ma^4b^2r\\
&-12Ma^2b^2r^3+12Mb^2r^5+3a^6b^2-9a^2b^2r^4\\
&-6b^2r^6+8M^3r+2Ma^2r-2Mr^3-a^4+r^4, \qquad \text{(A.9)}
\end{aligned}
$$

$$
\begin{aligned}
f^{(4)}_{(m)} &= -\Delta\Big(48M^3a^4b^6r-144M^4a^4b^6+288M^3a^2b^6r^3\\
&+16M^2a^6b^6+312M^2a^4b^6r^2+168M^2a^2b^6r^4\\
&-60Ma^6b^6r-120Ma^4b^6r^3-60Ma^2b^6r^5\\
&+4a^8b^6+6a^6b^6r^2-6a^4b^6r^4-14a^2b^6r^6-6b^6r^8\\
&+32M^4a^2b^4-24M^3a^2b^4r-56M^3b^4r^3\\
&-12M^2a^4b^4-180M^2a^2b^4r^2+72Ma^4b^4r\\
&+72Ma^2b^4r^3-9a^6b^4-9a^4b^4r^2\\
&+9a^2b^4r^4+9b^4r^6-4M^2a^2b^2\\
&-18Ma^2b^2r+6a^4b^2+3a^2b^2r^2-3b^2r^4-a^2\Big), \qquad \text{(A.10)}\\
f^{(6)}_{(m)} &= b^2\Delta\Big(96M^4a^4b^4-176M^3a^4b^4r-384M^3a^2b^4r^3\\
&+344M^2a^4b^4r^2+344M^2a^2b^4r^4-60Ma^6b^4r\\
&-120Ma^4b^4r^3-60Ma^2b^4r^5+6a^8b^4+14a^6b^4r^2\\
&+6a^4b^4r^4-6a^2b^4r^6-4b^4r^8-16M^4a^2b^2\\
&+24M^3a^2b^2r-8M^3b^2r^3+12M^2a^4b^2\\
&-84M^2a^2b^2r^2+48Ma^4b^2r+48Ma^2b^2r^3\\
&-9a^6b^2-15a^4b^2r^2-3a^2b^2r^4+3b^2r^6\\
&-6Ma^2r+3a^4+3a^2r^2\Big), \qquad \text{(A.11)}\\
f^{(8)}_{(m)} &= -b^4\Delta\Big(64M^3a^4b^2r-16M^4a^4b^2-104M^3a^2b^2r^3\\
&-8M^2a^6b^2+44M^2a^4b^2r^2+116M^2a^2b^2r^4\\
&-30Ma^6b^2r-60Ma^4b^2r^3-30Ma^2b^2r^5+4a^8b^2\\
&+11a^6b^2r^2+9a^4b^2r^4+a^2b^2r^6-b^2r^8-12M^2a^2r^2\\
&+12Ma^4r+12Ma^2r^3-3a^6-6a^4r^2-3a^2r^4\Big), \qquad \text{(A.12)}\\
f^{(10)}_{(m)} &= a^2b^6\Delta^4. \qquad \text{(A.13)}
\end{aligned}
$$

Finally, we present the term that effectively vanishes under the weak-field approximation in the radial equation (3.3). It includes corrections due to magnetization and black hole parameters up to high polynomial order.

$$
\begin{aligned}
f_{(0)} = -\frac{b^2q^2}{\Delta a^2}\Big\{&f^{(0)}_{(0)}+f^{(2)}_{(0)}\cos^2\theta+f^{(4)}_{(0)}\cos^4\theta\\
&+f^{(6)}_{(0)}\cos^6\theta+f^{(8)}_{(0)}\cos^8\theta+f^{(10)}_{(0)}\cos^{10}\theta\Big\},
\end{aligned} \qquad \text{(A.14)}
$$

where

$$
\begin{aligned}
f^{(0)}_{(0)} &= \left(2Ma^2+ra^2+r^3\right)\Big(20M^2a^6b^4r-8M^3a^6b^4\\
&-44M^2a^4b^4r^3+4Ma^8b^4+6Ma^6b^4r^2\\
&-2Ma^2b^4r^6+a^8b^4r+3a^6b^4r^3\\
&+3a^4b^4r^5+a^2b^4r^7+16M^3a^4b^2-48M^3a^2b^2r^2\\
&+8M^2a^4b^2r-4Ma^6b^2+4Ma^2b^2r^4\\
&-2a^6b^2r-4a^4b^2r^3-2a^2b^2r^5-16M^4r\\
&-2Ma^2r^2+ra^4+a^2r^3\Big), \qquad \text{(A.15)}\\
f^{(2)}_{(0)} &= 16M^4a^8b^4-576M^4a^6b^4r^2+240M^3a^8b^4r\\
&+384M^3a^6b^4r^3+144M^3a^4b^4r^5\\
&+24M^2a^8b^4r^2+48M^2a^6b^4r^4+24M^2a^4b^4r^6\\
&-32Ma^{10}b^4r-88Ma^8b^4r^3-72Ma^6b^4r^5\\
&-8Ma^4b^4r^7+8Ma^2b^4r^9+a^{12}b^4-10a^8b^4r^4\\
&-20a^6b^4r^6-15a^4b^4r^8-4a^2b^4r^{10}\\
&-192M^5a^4b^2r+64M^4a^6b^2+384M^4a^4b^2r^2\\
&+192M^4a^2b^2r^4-96M^3a^6b^2r-16M^3a^4b^2r^3\\
&-48M^3a^2b^2r^5-8M^2a^8b^2-144M^2a^6b^2r^2\\
&-136M^2a^4b^2r^4+36Ma^8b^2r+60Ma^6b^2r^3+12Ma^4b^2r^5\\
&-12Ma^2b^2r^7-2a^{10}b^2+12a^6b^2r^4+16a^4b^2r^6\\
&+6a^2b^2r^8+64M^5a^2r-16M^4a^4+16M^4r^4\\
&+12M^2a^4r^2-8Ma^6r-4Ma^4r^3+4Ma^2r^5\\
&+a^8-3a^4r^4-2a^2r^6, \qquad \text{(A.16)}\\
f^{(4)}_{(0)} &= -a^2\Delta\Big(48M^3a^4b^4r-144M^4a^4b^4-288M^3a^2b^4r^3\\
&+16M^2a^6b^4+312M^2a^4b^4r^2+168M^2a^2b^4r^4\\
&-60Ma^6b^4r-120Ma^4b^4r^3-60Ma^2b^4r^5\\
&+4a^8b^4+6a^6b^4r^2-6a^4b^4r^4-14a^2b^4r^6\\
&-6b^4r^8+64M^4a^2b^2-48M^3a^2b^2r-112M^3b^2r^3\\
&-8M^2a^4b^2-120M^2a^2b^2r^2+48Ma^4b^2r\\
&+48Ma^2b^2r^3-6a^6b^2-6a^4b^2r^2+6a^2b^2r^4\\
&+6b^2r^6-16M^4-6Ma^2r+2a^4+a^2r^2-r^4\Big), \qquad \text{(A.17)}\\
f^{(6)}_{(0)} &= a^2\Delta\Big(96M^4a^4b^4-176M^3a^4b^4r-384M^3a^2b^4r^3\\
&+344M^2a^4b^4r^2+344M^2a^2b^4r^4-60Ma^6b^4r\\
&-120Ma^4b^4r^3-60Ma^2b^4r^5+6a^8b^4+14a^6b^4r^2\\
&+6a^4b^4r^4-6a^2b^4r^6-4b^4r^8-32M^4a^2b^2\\
&+48M^3a^2b^2r-16M^3b^2r^3+8M^2a^4b^2\\
&-56M^2a^2b^2r^2+32Ma^4b^2r+32Ma^2b^2r^3-6a^6b^2\\
&-10a^4b^2r^2-2a^2b^2r^4+2b^2r^6-2Ma^2r+a^4+a^2r^2\Big), \qquad \text{(A.18)}\\
f^{(8)}_{(0)} &= -a^2b^2\Delta\Big(64M^3a^4b^2r-16M^4a^4b^2-104M^3a^2b^2r^3\\
&-8M^2a^6b^2+44M^2a^4b^2r^2+116M^2a^2b^2r^4\\
&-30Ma^6b^2r-60Ma^4b^2r^3-30Ma^2b^2r^5+4a^8b^2\\
&+11a^6b^2r^2+9a^4b^2r^4+a^2b^2r^6-b^2r^8\\
&-8M^2a^2r^2+8Ma^4r+8Ma^2r^3\\
&-2a^6-4a^4r^2-2a^2r^4\Big), \qquad \text{(A.19)}
\end{aligned}
$$

and

$$
f^{(10)}_{(0)} = a^4b^4\Delta^4. \qquad \text{(A.20)}
$$

B Double Confluent Heun structure and VBK method for Eq. (4.2)

The Double Confluent Heun (dCH) function, $H_D(\alpha, \beta, \gamma, \delta, z)$, is defined as the solution of a second-order ODE with two irregular singular points at $z = 0$ and $z = \infty$. It generalizes hypergeometric and confluent Heun functions and naturally arises in problems involving curved spacetimes, external fields, or quasi-exactly solvable potentials [39,40]. A canonical form of the dCH equation is

$$x^2u'' + (ax + b)\,u' + (Ax^2 + Bx + C + \tfrac{D}{x} + \tfrac{E}{x^2})\,u = 0. \tag{B.1}$$

Our radial equation (4.2) maps directly onto this structure upon the gauge transformation $R(x) = e^{\tau/x}u(x)$ with $\tau \in \mathbb{C}$, yielding the identifications

$$a = 2, \quad b = -2\tau, \quad A = h_2(\omega), \quad B = h_1(\omega),$$
$$C = h_0(\omega), \quad D = h_{-1}(\omega), \quad E = \tau^2.$$

Thus Eq. (4.2) is a genuine member of the dCH family, requiring no auxiliary constraints beyond the physical boundary conditions. This provides the analytic foundation for treating bound and quasibound states in the Melvin–Kerr background.

To extract the (quasi)bound-state frequencies we apply the continued-fraction method of Vieira, Bezerra, and Kokkotas (VBK) [42–44], adapted here to the gauged dCH form

$$x^2u'' + (2x - 2\tau)\,u' + \Big(Ax^2 + Bx + C + \tfrac{D}{x} + \tfrac{E}{x^2}\Big)\,u = 0, \tag{B.2}$$

with (A, B, C, D, E) as above. Choosing $\tau = i\,\eta_H(\omega)$ ensures regularity at the horizon and automatically selects the ingoing branch. Near the horizon ($x = 0$), the solution admits a Frobenius expansion

$$u(x) = x^s \sum_{n=0}^{\infty} a_n x^n, \qquad a_0 \neq 0, \tag{B.3}$$

with indicial exponent $s = \tau$. Substituting into Eq. (B.2) yields a five-term recurrence,

$$A\,a_{n-2} + B\,a_{n-1} + \big[(n+s)^2 + (n+s) + C\big]a_n + \big[D - 2\tau(n+1+s)\big]a_{n+1} + E\,a_{n+2} = 0, \tag{B.4}$$

valid for $n \geq 0$ with $a_{-1} = a_{-2} = 0$. This can be reduced by Gaussian elimination to a three-term form

$$\alpha_n(\omega)\,a_{n+1} + \beta_n(\omega)\,a_n + \gamma_n(\omega)\,a_{n-1} = 0 \qquad (n \geq 1), \tag{B.5}$$

whose minimal solution, identified by a Pincherle continued fraction,

$$\frac{a_1}{a_0} = -\frac{\beta_0}{\alpha_0} - \frac{\gamma_1}{\alpha_0}\,\cfrac{1}{\frac{\beta_1}{\alpha_1} - \cfrac{\gamma_2}{\frac{\beta_2}{\alpha_2} - \cfrac{\gamma_3}{\ddots}}}, \tag{B.6}$$

selects the purely ingoing solution at the horizon.

At spatial infinity the solution behaves as a Thomé-type series,

$$R(x) \sim \frac{1}{x}\,\exp\big(-M\kappa_\infty(\omega)\,x\big)\sum_{n=0}^{\infty} b_n x^{-n},$$
$$\kappa_\infty(\omega) = \sqrt{\mu^2 - \omega^2 - \frac{2qb}{a}\big(am - 4M^2\omega\big)}, \tag{B.7}$$

which guarantees exponential decay provided $\Re\,\kappa_\infty(\omega) > 0$. The coefficients b_n again satisfy a finite-band recurrence reducible to a three-term continued fraction, from which the decaying branch is isolated. The spectrum follows by matching the ingoing and decaying solutions at some intermediate $x_* > 0$. This is implemented by equating their logarithmic derivatives, yielding the master equation

$$\mathcal{F}(\omega) = \mathcal{L}_{\rm in}(\omega; x_*) - \mathcal{L}_\infty(\omega; x_*) = 0, \tag{B.8}$$

whose roots give the discrete (quasi)bound-state frequencies. Above, $\mathcal{L}(\omega; x) \equiv u'(x)/u(x)$ denotes the logarithmic derivative of the local solution. In practice, $K_{lm}(\omega)$ is updated at each trial ω. For weak magnetic fields we employ the perturbative expression (3.16), while higher accuracy can be obtained by solving the angular equation numerically.

References

1. R. Penrose, R.M. Floyd, Extraction of rotational energy from a black hole. Nature **229**, 177–179 (1971)
2. W.H. Press, S.A. Teukolsky, Floating orbits, superradiant scattering and the black-hole bomb. Nature **238**, 211–212 (1972)
3. Y.B. Zel'dovich, Generation of waves by a rotating body. JETP Lett. **14**, 4 (1971)
4. S. Hod, Stationary scalar clouds around rotating black holes. Phys. Rev. D **86**, 104026 (2012)
5. S. Hod, Kerr–Newman black holes with stationary charged scalar clouds. Phys. Rev. D **90**(2), 024051 (2014)
6. C.A.R. Herdeiro, E. Radu, Kerr black holes with scalar hair. Phys. Rev. Lett. **112**, 221101 (2014)
7. C.L. Benone, L.C.B. Crispino, C. Herdeiro, E. Radu, Kerr–Newman scalar clouds. Phys. Rev. D **90**(10), 104024 (2014)
8. N.M. Santos, C.A.R. Herdeiro, Stationary scalar and vector clouds around Kerr–Newman black holes. Int. J. Mod. Phys. D **29**(11), 2041013 (2020)
9. X. Qiao, M. Wang, Q. Pan, J. Jing, Kerr–Mog black holes with stationary scalar clouds. Eur. Phys. J. C **80**(6), 509 (2020)
10. S. Hod, Analytic treatment of near-extremal charged black holes supporting non-minimally coupled massless scalar clouds. Eur. Phys. J. C **80**(12), 1150 (2020)

11. Y. Brihaye, B. Hartmann, Born–Infeld stars and charged black holes surrounded by scalar clouds. Phys. Rev. D **110**(8), 084006 (2024)
12. C. Bernard, Stationary charged scalar clouds around black holes in string theory. Phys. Rev. D **94**(8), 085007 (2016)
13. A. Arvanitaki, S. Dubovsky, Exploring the string axiverse with precision black hole physics. Phys. Rev. D **83**, 044026 (2011)
14. R. Brito, V. Cardoso, P. Pani, Superradiance: new frontiers in black hole physics. Lect. Notes Phys. **906**(2015), 1–237 (2020)
15. H. Yoshino, H. Kodama, Probing the string axiverse by gravitational waves from cygnus x-1. PTEP **6**, 061E01 (2015)
16. R. Brito, S. Shah, Extreme mass-ratio inspirals into black holes surrounded by scalar clouds. Phys. Rev. D **108**(8), 084019 (2023)
17. S. Hod, Stationary scalar clouds supported by rapidly-rotating acoustic black holes in a photon-fluid model. Phys. Rev. D **103**(8), 084003 (2021)
18. M. Ciszak, F. Marino, Acoustic black-hole bombs and scalar clouds in a photon-fluid model. Phys. Rev. D **103**(4), 045004 (2021)
19. K. Akiyama et al., [Event Lorizon Telescope], First m87 event horizon telescope results. VIII. Magnetic field structure near the event horizon. Astrophys. J. Lett. **910**(1), L13 (2021)
20. F.J. Ernst, Black holes in a magnetic universe. J. Math. Phys. **17**(1), 54–56 (1976)
21. V. Karas, Z. Stuchlik, Magnetized black holes: interplay between charge and rotation. Universe **9**(6), 267 (2023)
22. A.N. Aliev, D.V. Galtsov, Radiation from relativistic particle in nongeodesic motion in a strong gravitational field. Gen. Relativ. Gravit. **13**, 899–912 (1981)
23. R. Brito, V. Cardoso, P. Pani, Superradiant instability of black holes immersed in a magnetic field. Phys. Rev. D **89**(10), 104045 (2014)
24. R.A. Konoplya, Magnetic field creates strong superradiant instability. Phys. Lett. B **666**, 283–287 (2008)
25. N.M. Santos, C.A.R. Herdeiro, Black holes, stationary clouds and magnetic fields. Phys. Lett. B **815**, 136142 (2021)
26. D. Yang, W. Liu, X. Wu, Impact of electric charges on chaos in magnetized Reissner–Nordström spacetimes. Eur. Phys. J. C **83**(5), 357 (2023)
27. H.C.D.L. Junior, P.V.P. Cunha, C.A.R. Herdeiro, L.C.B. Crispino, Shadows and lensing of black holes immersed in strong magnetic fields. Phys. Rev. D **104**(4), 044018 (2021)
28. R.A. Konoplya, Magnetized black hole as a gravitational lens. Phys. Lett. B **644**, 219–223 (2007)
29. R.A. Konoplya, R.D.B. Fontana, Quasinormal modes of black holes immersed in a strong magnetic field. Phys. Lett. B **659**, 375–379 (2008)
30. H.M. Siahaan, Magnetized Taub-NUT spacetime. Nucl. Phys. B **978**, 115741 (2022)
31. H.M. Siahaan, Textitmagnetized Reissner–Nordström–Taub–NUT spacetime and microscopic entropy. Eur. Phys. J. C **81**(9), 838 (2021)
32. H.M. Siahaan, Magnetized Kerr–Taub-NUT spacetime and Kerr/CFT correspondence. Phys. Lett. B **820**, 136568 (2021)
33. M. Ghezelbash, H.M. Siahaan, Magnetized Kerr–Newman–Taub-Nut spacetimes. Eur. Phys. J. C **81**(7), 621 (2021)
34. M. Ghezelbash, H.M. Siahaan, Meissner effect and holographic dual for the Melvin–Kerr–Newman–Taub-NUT spacetimes. Eur. Phys. J. C **83**(5), 448 (2023)
35. H.M. Siahaan, B.J. Bansawang, T. Surungan, P.C. Tjiang, Properties of Melvin–Taub-NUT spacetime with Manko–Ruiz parameter. Gen. Relativ. Gravit. **55**(10), 113 (2023)
36. G.W. Gibbons, Y. Pang, C.N. Pope, Thermodynamics of magnetized Kerr–Newman black holes. Phys. Rev. D **89**(4), 044029 (2014)
37. G.W. Gibbons, A.H. Mujtaba, C.N. Pope, Ergoregions in magnetised black hole spacetimes. Class. Quantum Gravity **30**(12), 125008 (2013)
38. I. Booth, M. Hunt, A. Palomo-Lozano, H.K. Kunduri, Insights from Melvin–Kerr–Newman spacetimes. Class. Quantum Gravity **32**(23), 235025 (2015)
39. A. Ronveaux, F.M. Arscott, *Heun's Differential Equations* (Oxford University Press, Oxford, 1995)
40. S.Yu. Slavyanov, W. Lay, *Special Functions: A Unified Theory Based on Singularities* (Oxford University Press, Oxford, 2000)
41. M. Abramowitz, I.A. Stegun, *Handbook of Mathematical Functions with Formulas, Graphs, and Mathematical Tables* (Dover, New York City, 1964)
42. H.S. Vieira, V.B. Bezerra, Resonant frequencies of a massless scalar field in the canonical acoustic black hole spacetime. Gen. Relativ. Gravit. **52**(8), 72 (2020)
43. H.S. Vieira, K. Destounis, K.D. Kokkotas, Slowly-rotating curved acoustic black holes: quasinormal modes, Hawking–Unruh radiation, and quasibound states. Phys. Rev. D **105**(4), 045015 (2022)
44. H.S. Vieira, K.D. Kokkotas, Quasibound states of Schwarzschild acoustic black holes. Phys. Rev. D **104**(2), 024035 (2021)
45. S. Hod, Nonequatorial scalar clouds supported by maximally spinning Kerr black holes. Phys. Rev. D **108**(12), 124028 (2023)
46. Y.H. Lei, Z.H. Yang, X.M. Kuang, Scalar field perturbation around a rotating hairy black hole: quasinormal modes, quasibound states and superradiant instability. Eur. Phys. J. C **84**(4), 438 (2024)
47. S. Hod, Spatially regular charged black holes supporting charged massive scalar clouds. Phys. Rev. D **109**(6), 064074 (2024)
48. T.J.M. Zouros, D.M. Eardley, Instabilities of massive scalar perturbations of a rotating black hole. Ann. Phys. **118**, 139–155 (1979)
49. H.S. Vieira, K. Destounis, K.D. Kokkotas, Perturbing the vortex: quasinormal and quasibound spectra of rotating acoustic geometries. Phys. Rev. D **111**(10), 104025 (2025)